Weight Comparisons of Optimized Stiffened, Unstiffened, and Sandwich Cylindrical Shells

B. L. Agarwal*
Northrop Corp., Hawthorne, Calif.
and
L. H. Sobel†
Westinghouse Electric Corp., Madison, Pa.

This work presents optimum designs for unstiffened, hat-stringer-stiffened, and honeycomb sandwich cylinders under axial compression. Optimization results for graphite-epoxy cylinders show approximately a 50% weight savings over corresponding optimized aluminum cylinders for a wide loading range. The inclusion of minimum gage considerations results in a significant weight penalty, especially for a lightly loaded cylinder. Effects of employing a smeared stiffener buckling theory in the optimization program are investigated through comparison of results obtained from a more accurate branched shell buckling computer code. It was found that the stiffener cross-sectional deformations, which are usually ignored in smeared stiffener theory, result in a reduction of buckling load by 30% for the graphite-epoxy hat stiffened cylinder.

Nomenclature

A_s = cross-sectional area of stringer
A_{ij} = elements of extensional stiffness matrix
D_{ij} = elements of bending stiffness matrix
E_s = Young's modulus of stringer
EA_i = extensional stiffness of ith plate element of the stiffener (see Fig. 2)
E_x = lamina modulus in the filament direction
E_y = lamina modulus transverse to the filament direction
G_s = shear modulus of stringer
GJ_{eff} = effective torsional stiffness of stringer
G_{xy} = lamina inplane shear modulus
I_{os} = moment of inertia of stringer about middle surface of shell
J_s = torsional constant for stringer
L = length of stiffened cylinder
$\bar{N}_x, \bar{N}_y$ = applied compressive loads
$\bar{N}_x/R$ = loading index
$\bar{z}_s$ = distance from the neutral axis of stringer to the middle surface of orthotropic shell (see Fig. 1); positive if stiffener lies on external surface of the shell.
α_i = orientation of ith lamina in the cylinder skin (see Fig. 1): $\alpha_1 = 0$ corresponds to a fiber in the axial direction
ρ = material density
$\epsilon_{xc}, \epsilon_{yc}, \gamma_{xyc}$ = material yield strains
μ_{xy} = transverse Poisson's ratio of lamina
R = middle surface radius of the cylinder
W = weight per unit area of the stiffened cylinder
W_0 = weight corresponding to the total torsional stiffness of the stringer (see Fig. 8)
W/R = weight parameter for the cylinders
b_s = width of the stringer (see Fig. 2)
b_i = width of the ith element of stiffener (see Fig. 2)
h_s = depth of the stringer (see Fig. 2)
i,j = indices
l_s = stringer spacing
m = number of half waves in the cylinder buckle pattern in the longitudinal direction
n = number of full waves in the cylinder buckle pattern in the circumferential direction
t = laminate thickness
t_i = thickness of ith layer in the cylinder skin (see Fig. 1)
t_{1s}, t_{2s}, t_{3s} = thickness of stringer geometry (see Fig. 2)

Presented at the AIAA/ASME/SAE 17th Structures, Structural Dynamics, and Materials Conference, King of Prussia, Pa., May 5-7, 1976 (in bound volume of Conference papers, no paper number); submitted May 7, 1976; revision received June 13, 1977.

Index categories: Structural Design; Structural Stability; Structural Composite Materials.

*Senior Engineer. Member AIAA.

†Principal Engineer. Formerly with the University of Cincinnati. Member AIAA.

I. Introduction

THE need for highly efficient structures in the aerospace industry led to the development of fiber-reinforced composite materials. The low density and high stiffness of these materials, relative to conventional aerospace metals, indicated that they would be highly efficient as compression members, and that the optimum proportions of such structures should be investigated.

In Refs. 1 and 2, the minimum weight design of stiffened composite flat panels under axial compression was investigated. Over a wide loading range, the results of those investigations show that about a 50% weight reduction could be achieved for axially compressed graphite/epoxy hat-stiffened panels in comparison with aluminum panels. Several panels were tested at the NASA Langley Research Center and very favorable correlations between test and theory have been found.[3] The present investigation extends the work of Refs. 1 and 2 to the minimum weight design of hat stringer-stiffened and unstiffened composite cylindrical shells subjected to axial compression.

Past investigators[4-6] have used various techniques to determine the optimum proportions for structural members constructed from conventional isotropic metals. These techniques, for a number of reasons, are insufficient for the optimum design of composite structural elements. Unlike conventional metals, filamentary reinforced composite materials are orthotropic, or even anisotropic. Furthermore, the full determination of the appropriate form and optimum proportions of the structural members constructed from these materials requires consideration of a significantly larger number of design variables than those needed for the case of isotropic materials. The reduction in the number of design variables, through the use of undue restrictions in the optimization procedure, denies the designer many of the ad-

vantages offered by composite materials. Therefore, in the present work, the optimum proportions of composite-stiffened and unstiffened cylinders are obtained through the use of an optimization technique that can properly accommodate a large number of design variables.

Mathematical programming has been shown to be a very effective technique for the optimization of structural problems involving a large number of design variables.[7-9] For the case of flat panels, it was shown in Refs. 1 and 2 that multiple optimum designs can be obtained for composites and mathematical programming was best suited for this purpose. Hence, in the present study, a computer code based on a nonlinear mathematical programming technique, called AESOP (Automated Engineering and Scientific Optimization Program[10]), is used in conjunction with a mathematical model of a stiffened cylinder to determine optimum composite cylinder designs.

The specific problem considered herein is the optimization of composite-stiffened, and unstiffened cylindrical shells under uniaxial compression. The loaded edges are assumed to be simply supported. The following three basic configurations (see Fig. 1) are used for the present study: 1) an unstiffened cylinder, 2) a sandwich wall cylinder, and 3) a hat-stringer-stiffened cylinder. The optimized results for these composite configurations are compared with those appropriate to corresponding aluminum configurations. The material properties used in this study are given in Table 1.

The mathematical model of the stiffened cylinder includes both stability and strength considerations. Local buckling loads for the stiffener components are determined from orthotropic plate theory. Gross and skin buckling loads are determined from "smeared" cylindrical shell theory, which accounts for the effects of stiffener eccentricity.[11] The results from smeared theory are compared with the results obtained from the BUCLASP-2 computer code,[12] which is based on a more exact branched shell theory. As a consequence of this comparison, appropriate modifications are made in the smeared theory to effect good correlation. Maximum strain theory is used to describe the load-carrying capacity of the laminae, and each lamina is checked for failure.

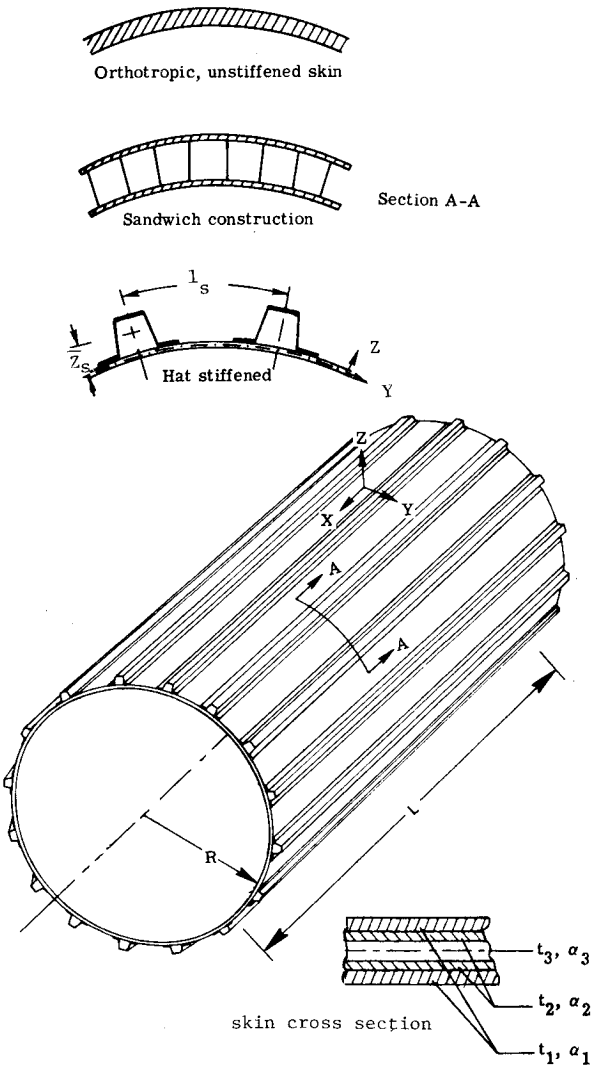

Fig. 1 Cylinder and skin notations.

II. Method of Analysis

The synthesis process consists of two parts, namely, the mathematical model and the optimizer. The mathematical model defines the design variables and describes the strength and stability requirements for the structure to be optimized. The weight per unit surface area (performance function) is evaluated for the design variables and checked for a minimum. The design variables are incremented, in accordance with the optimization scheme, subject to various design constraints, and the process is repeated until an optimum design has been generated. Details of the optimization scheme are given in Ref. 13. The remainder of this section presents a discussion of the design variables and the design constraints.

A. Design Variables

In order to determine a suitable mathematical model for the type of structure shown in Fig. 1, it is important, of course, to define properly the design variables. The judicious selection of these design variables can result in a less restrictive structural configuration and better optimum designs.

The loading, radius, and length of the cylinder are assumed to be known parameters. The length was assumed to be 30 in., which is typical of the ring spacing for stiffened aerospace cylinders. The cross-sectional dimensions and lamina orientations are the design variables for the optimization process. The cylinder to be optimized is shown in Fig. 1. It is assumed that the stringer spacing l_s is an unknown design variable. The skin of the cylinder is allowed to have three different lamina orientations, α_1, α_2, and α_3, which are assumed to be completely arbitrary. The corresponding lamina thicknesses are t_1, t_2, and t_3. The skin is assumed to be orthotropic, and each layer is balanced. This arrangement of skin variables allows a very general unstiffened cylindrical shell configuration that can be used for optimization purposes and, with the proper values of material constants in each lamina, a sandwich wall construction can be achieved. For example, laminae 1 and 2 would be made of graphite/epoxy and lamina 3 would be made of honeycomb material. It should also be noted that in the present sandwich con-

Table 1 Material properties

Material	E_x, ksi	E_y, ksi	G_{xy}, ksi	μ_{xy}	ρ, lb/in.^{3}	ϵ_{xc}	ϵ_{yc}	γ_{xyc}
Graphite/epoxy	21,200	2390	650	0.31	0.055	0.012	0.0075	0.015
Aluminum	10,000	10,000	3850	0.33	0.10	0.006	0.006	0.015
Aluminum honeycomb	0.001	0.001	0.001	0.10	0.001736	0.012	0.0075	0.015
Glass-reinforced	7501	2229	879	0.224	0.079	0.012	0.0075	0.015

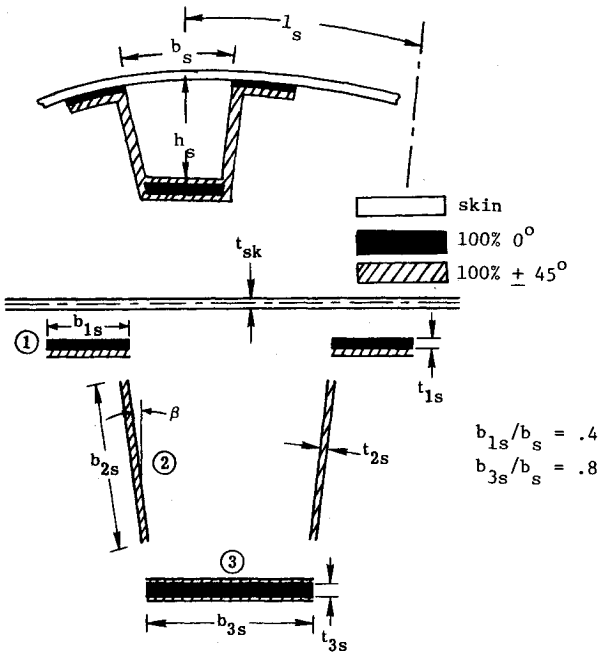

Fig. 2 Stringer elemental details and notation.

struction, the weight of the adhesive is not taken int account and an aluminum honeycomb core of density $\rho = 3$ lb/ft^3 is used. A midplane symmetry of the wall construction for both the unstiffened and sandwich configuration is assumed. Thus, so far, there are a total of seven design variables (l_s, α_i, t_i, $i = 1,2,3$) as shown in Fig. 1.

A sketch of the stringer is shown in Fig. 2. The stringer is assumed to behave as a one-dimensional member. At this point, results previously obtained for the composite stiffened flat plate[1,2] are used to reduce the number of design variables. It was shown that, for an optimum stiffener design, the lamina orientations should be as depicted in Fig. 2 and also that the panel weight is very insensitive to certain design variables. It is assumed that b_s and h_s are the basic design variables that determine the size of the stiffener. From the results of Refs. 1 and 2, b_{1s} and b_{3s} are assumed to be $0.4b_s$ and $0.8b_s$, resepectively, as these values result in practical stiffener cross sections. Thus, there are five design variables (b_s, h_s, t_{1s}, t_{2s}, t_{3s}) for the stringer. Hence, a total of twelve design variables are used to define a general mathematical model of the three basic configurations under study.

B. Design Constraints

There are primarily two kinds of design constraints for the problem under consideration, namely, stability and strength constraints, as an optimum design should be void of instability and material failure.

To insure the stability of the cylinder, the following three types of buckling modes are considered: 1) gross buckling; 2) skin buckling (buckling of skin between stringers); 3) local buckling of stringers. For the purpose of calculation of the constraints due to skin buckling and the local buckling of the stringers, the load distribution in the stiffened cylinder element is determined through the use of a membrane prebuckling stress analysis.[13]

The strength requirements for the design are satisfied by the use of a maximum strain theory. Each lamina in the structure is checked for strain limits, and the design strains are constrained to be lower than limit strains.

General Instability

The judicious selection of a suitable buckling analysis of composite-stiffened cylinders is very important with regard to the consideration of achieving an economical solution, as the optimization scheme used for this purpose is of an iterative nature. It has been customary to use a smeared-stiffener theory for the prediction of buckling loads for the stiffened cylinders. For the present study, the smeared theory presented by Block et al.[11] is modified to account for the laminated wall construction of the composite cylinder and stiffeners. Bushnell[14] points out that the cross-sectional deformations of the stiffeners can be important for aluminum stiffened cylindrical panels. Hence, to check the adequacy of the smeared-stiffener theory, a comparison of the results obtained therefrom is made with those appropriate to a more exact (branched shell) theory which is used in the BUCLASP-2 computer program.[12]

The following assumptions are made in the development of the smeared-stiffener theory for the stiffened cylinder shown in Fig. 1.

1) The stiffened cylinder is composed of an orthotropic skin which is stiffened by identical and equally spaced stringers.

2) The stringers are assumed to be closely spaced so that their elastic properties can be averaged (smeared) over the stringer spacing.

3) Donnell-type shell theory is used and the stiffeners are treated as one-dimensional beam members with stiffener twisting accounted for in an approximate manner to be described later.

With the above assumptions, the theory of Block et al.[11] is modified in Ref. 13 to account for the laminated wall construction of the cylinder, and the resulting equation for the general instability load $\bar{N}_x$ is given by

$$\bar{N}_x = \frac{K_{33} + \dfrac{K_{12}K_{23} - K_{13}K_{22}}{K_{11}K_{22} - K_{12}^2} K_{13} + \dfrac{K_{12}K_{13} - K_{11}K_{23}}{K_{11}K_{22} - K_{12}^2} K_{23}}{(m\pi/L)^2 + (\bar{N}_y/\bar{N}_x)(n/R)^2} \tag{1}$$

where

$$K_{11} = [A_{11} + (E_sA_s/l_s)](m\pi/L)^2 + A_{66}(n/R)^2$$

$$K_{12} = [A_{12} + A_{66}](m\pi/L)(n/R)^2$$

$$K_{13} = A_{12}(m\pi/L)(1/R) + (E_sA_s\bar{z}_s/l_s)(m\pi/L)^3$$

$$K_{22} = A_{66}(m\pi/L)^2 + A_{22}(n/R)^2$$

$$K_{23} = A_{22}(n/R)(1/R)$$

$$K_{33} = \left[D_{11} + \frac{E_sI_{os}}{l_s}\right]\left(\frac{m\pi}{L}\right)^4 + \left[2(D_{12} + 2D_{66}) + \frac{G_sJ_s}{l_s}\right] \times \left(\frac{m\pi}{L}\right)^2\left(\frac{n}{R}\right)^2 + D_{22}\left(\frac{n}{R}\right)^4 + A_{22}\left(\frac{1}{R}\right)^2$$

The minimum value of $\bar{N}_x$ with varying m and n, for a fixed value of $\bar{N}_y/\bar{N}_x$, gives the buckling load. Equation (1) requires that the stiffness properties of the stringers be known. These stiffness properties are given in the Appendix.

Skin Buckling

With the use of Eq. (1), the gross and skin buckling loads are predicted as follows. For the gross buckling mode, Eq. (1) is used as presented, and for the skin buckling mode, all the terms due to stringer stiffness are set equal to zero and the minimum buckling load corresponds to

$$n = \text{integer } (\pi R/l_s)\bar{n} \qquad (\bar{n} = 1,2,3\ldots)$$

Local Buckling

For the local buckling of the stringers, the buckling of elements 2,3 and the skin between the webs is considered (see Fig. 4). All the stiffener elements are assumed to be or-

Table 2 Comparison of the results of Ref. 17 with the present results for unstiffened fiber glass-reinforced plastic cylinder under axial compression

$(W/R) \times 10^4$, lb/in^3	5.651	4.898	3.995	3.097	2.530	2.191	1.789
$(\bar{N}_x/R)$ present, psi	100	75	50	30	20	15	10
$(\bar{N}_x/R)$ Ref. 17, psi	121.3	91.1	60.61	36.42	24.31	18.23	12.15
% Error	21.3	21.46	21.2	21.4	21.55	21.53	21.5

Table 3 Optimized graphite/epoxy unstiffened cylindrical shell under axial compression

a) $\alpha_1 = 0°$, $\alpha_2 = 45°$, $\alpha_3 = 90°$, $t_1 = t_3 = t_2/2$							
$(\bar{N}_x/R)$, psi	100	75	50	30	20	15	10
$(W/R) \times 10^4$, lb/in^3	2.814	2.458	1.999	1.563	1.269	1.107	0.903
t_1, in.	0.0256	0.0223	0.0182	0.0142	0.0115	0.0101	0.0082
b) $\alpha_1 = 90°$, $\alpha_2 = 45°$, $\alpha_3 = 0°$, $t_1 = t_3 = t_2/2$							
$(\bar{N}_x/R)$, psi	100	75	50	30	20	15	10
$(W/R) \times 10^4$, lb/in^3	2.911	2.520	2.058	1.594	1.302	1.127	0.920
t_1, in.	0.0265	0.0229	0.0187	0.0145	0.0118	0.0102	0.0084
c) $\alpha_2 = \alpha_3 = t_2 = t_3 = 0$							
$(\bar{N}_x/R)$, psi	100	75	50	30	20	15	10
$(W/R) \times 10^4$, lb/in.^{3}	2.873	2.489	2.046	1.573	1.283	1.113	0.905
α_1, deg	72	73	73	73	17	17	17
t_1, in.	0.1044	0.0905	0.0744	0.0572	0.0467	0.0404	0.0329

thotropic plates that are simply supported on all four edges. Hence, the buckling load for ith member[15] is given by

$$\bar{P}_{xi} = (2\pi^2/b_i)\,(\sqrt{D_{11}D_{22}} + D_{12} + 2D_{66})_i \qquad (2)$$

where $\bar{P}_{xi}$ is the total buckling load, and b_i is the width of the plate member.

Strength Analysis

A maximum strain theory is used for the strength requirement of the cylinder. To use this theory, the strain in each individual lamina is calculated by transforming the laminate strain in the direction of the lamina. Then the lamina strain is constrained to be within the required allowable strains.

III. Numerical Results

A. Unstiffened Cylinders

As previously mentioned, the buckling analysis of Ref. 11 was modified in the present work to account for the laminated wall construction. The results of the modified theory were checked against results appropriate to the corresponding theory of BUCLAP-2,[16] and total agreement was found.

Table 2 shows a comparison of the present results with those given in Ref. 17 for a glass-reinforced plastic cylinder of an "isotropic" configuration. An isotropic configuration is defined as a fiber arrangement that results in an extensional stiffness matrix derived from only two independent material constants. The results presented in Table 2 are based on the equations for an isotropic configuration of Ref. 17 and the indicated values of the weight parameter W/R. Inspection of Table 2 reveals that there is considerable difference between the present results and those of Ref. 17. In Ref. 17, the effects of laminated construction were neglected in the computation of the bending stiffnesses of the laminate. The results in Table 2 indicate that these effects are important and can result in an error of approximately 20%.

Results for graphite/epoxy and glass-reinforced-plastic cylindrical shells are shown in Fig. 3. In both cases, the present "general" configuration depicted in Fig. 1 weighs less than the isotropic configuration. The general configuration is defined herein as one in which all the lamina orientations and

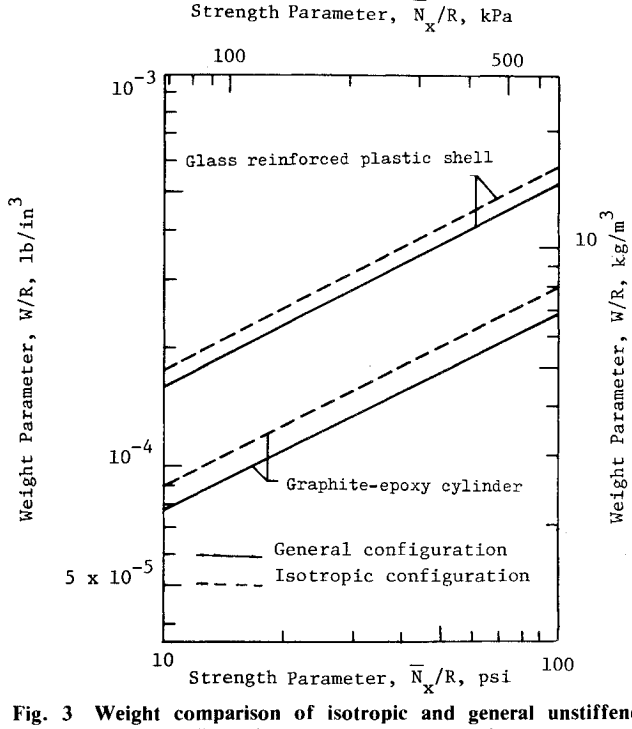

Fig. 3 Weight comparison of isotropic and general unstiffened cylindrical shell configuration, under axial compression.

thicknesses are determined according to the present optimization scheme. The general configuration graphite/epoxy and glass-reinforced plastic cylinders are approximately 15% and 10% lighter than their respective isotropic configurations. Table 3 presents weight results for two similar isotropic configurations (0°, ±45°, 90°, ∓45°, 0° and 90°, ±45°, 0°, ∓45°, 90°). In one case the 0° lamina is the outermost lamina and in the other case the 90° lamina is the outermost lamina. The results indicate approximately a 3% difference in the weight parameter W/R in the above cases. Table 3c presents results for a $\pm\alpha$ configuration graphite/epoxy cylinder. The weight parameters for the isotropic configuration and the optimized $\pm\alpha$ configuration are almost identical. However, it

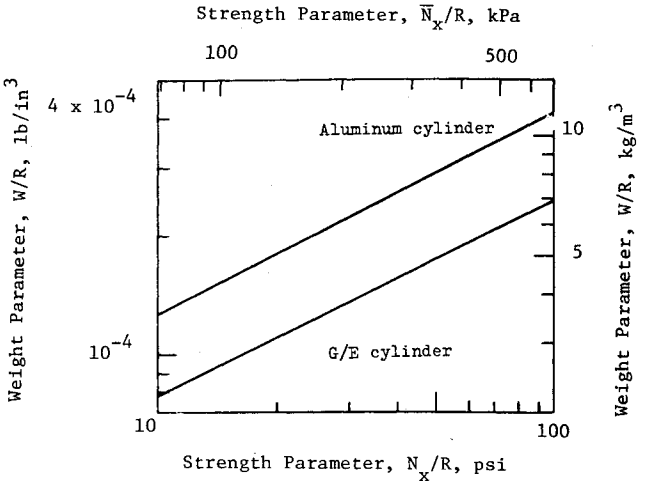

Fig. 4 Weight-strength plot for unstiffened cylinder under axial compression.

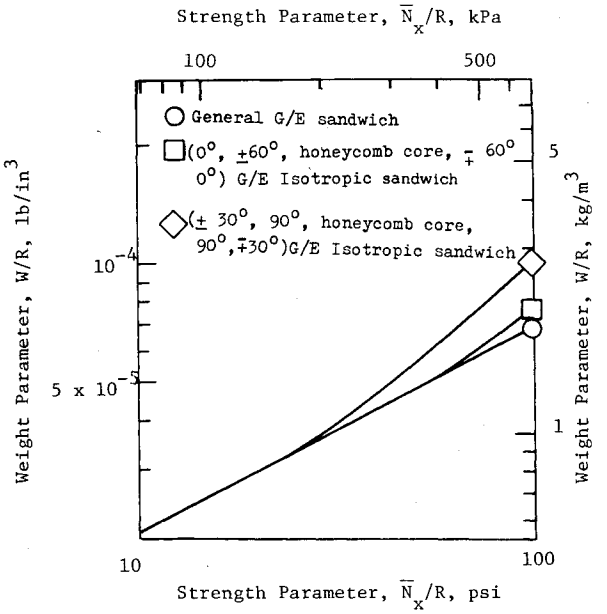

Fig. 5 Weight-strength comparison of three different graphite/epoxy sandwich constructions for a cylinder under axial compression.

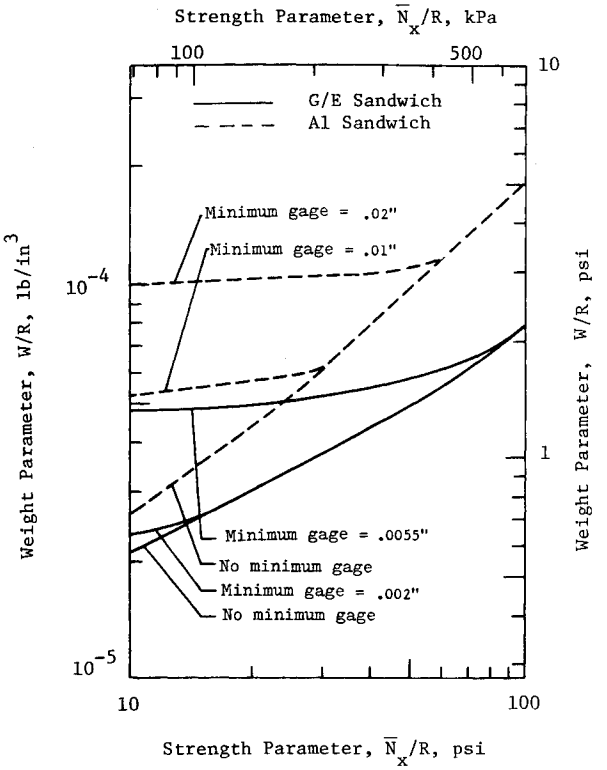

Fig. 6 Comparison of weight for some practically constrained honeycomb shells under axial compression.

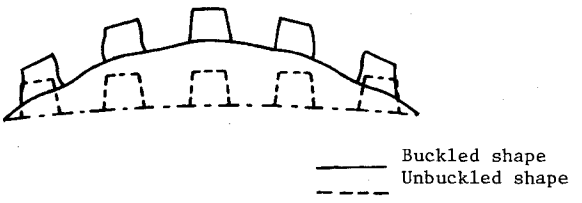

Fig. 7 A typical buckled and unbuckled shape of a stringer-stiffened cylinder under axial compression, branch shell theory.

is noted that the manufacture of a $\pm\alpha$ cylinder is considerably easier than that of an isotropic composite configuration, as a $\pm\alpha$ configuration requires only two different lamina orientations as compared to four for an isotropic configuration. Hence, the $\pm\alpha$ configuration is better from a manufacturing point of view.

Figure 4 shows weight-strength plots for an unstiffened graphite/epoxy cylinder and an aluminum cylinder. From this figure, it is observed that the graphite epoxy cylinder is about 40% lighter than the aluminum cylinder.

B. Honeycomb Sandwich Cylinders

Weight-strength plots for three different graphite/epoxy sandwich constructions are presented in Fig. 5. It is seen from Fig. 5 that the general sandwich construction is lighter than both isotropic configurations in the higher loading range, where the differences in the weight parameter occur. The reason for the differences stems primarily from the strain carrying capability of the various laminae. The general configuration can adjust the lamina orientations such that the laminae satisfy the limit strain values.

Figure 6 shows weight-strength results for isotropic (0°, ±60°, honeycomb core, ∓60°, 0°) graphite/epoxy sandwich and aluminum sandwich cylinders with and without the requirements of various minimum gage constraints imposed in the optimization procedure. The graphite/epoxy laminae are usually available in 0.002 and 0.0055 in. thicknesses and, for an isotropic construction, at least six laminae are required, whereas minimum gage aluminum sheets usually are available in 0.02 in. thickness. The minimum gage constraint imposes a considerable weight penalty, especially for the lightly loaded cylinders, as may be seen in Fig. 6. If commonly used graphite/epoxy tape and aluminum sheets are used (0.0055-in. graphite epoxy tape, 0.02-in. aluminum sheets), the graphite/epoxy honeycomb cylinders will weigh almost half as much as the aluminum sandwich cylinders subjected to the same axial compression.

C. Stringer-Stiffened Cylinders

The gross buckling analysis discussed earilier is used herein for the purpose of the present optimization study, and its validity is established by the comparison of the present results with those obtained from two computer programs, namely, BUCLAP-2, and BUCLASP-2.

The computer code BUCLAP-2 was used to check the modification made to the theory of Ref. 11, and the results of BUCLAP-2 and present theory are in complete agreement.

The BUCLASP-2 branched shell program was used to check the effects of smeared stiffener theory, which is used herein for the purpose of optimization. Several optimum designs were obtained based on smeared theory and the

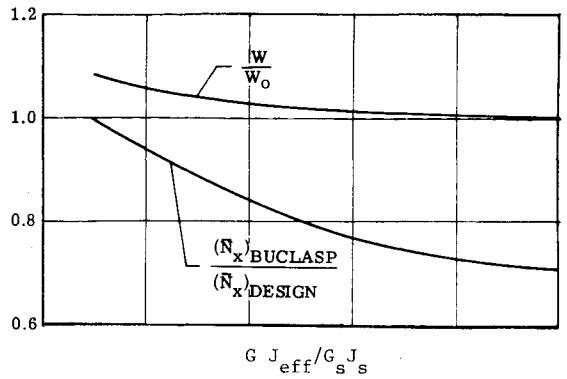

Fig. 8 Effect of reducing torsional stiffness on the weight and buckling load of a graphite/epoxy externally stiffened cylinder under axial compression ($\bar{N}_x = 300$ lb/in., $L = 30$ in., $R = 40$ in.).

buckling loads for these optimum designs were computed by the use of BUCLASP-2. The buckling loads predicted by BUCLASP-2 are about 30% lower than those predicted by the smeared theory for the graphite/epoxy cylinder. A typical buckling mode shape obtained from BUCLASP-2 is shown in Fig. 7. It can be seen in Fig. 7 that the stringers and skin deform locally. The local deformation of the stringers reduces the effective torsional stiffness of the stringer. Such stiffener deformations are omitted in the smeared theory used for the purpose of optimization. A study was made to account, approximately, for these local stringer deformations in the smeared theory. The variation of the ratio of load predicted by BUCLASP-2 to the design load (N_x BUCLASP/N_x DESIGN) with the reduction of the stringer torsional stiffness GJ_{eff}/G_sJ_s is shown in Fig. 8. The use of a reduction factor of 0.1 (or an effective torsional stiffness of $G_sJ_s/10$) in the smeared theory can approximately take into account the stringer deformations for the case presented. This reduction factor was found to be valid for both externally and internally stiffened graphite/epoxy cylinders over a wide loading range, but in general this reduction factor may vary. However, for aluminum-stiffened cylinders, reduction factors of, respectively, 0.5 and 0.6 were found to be suitable for the externally and internally stiffened cylinders. The increase in weight of the graphite/epoxy cylinder as a result of the reduction in torsional stiffness is also shown in Fig. 8. For the case presented, a weight penalty of 8% was imposed to account for the 30% increase in the buckling load.

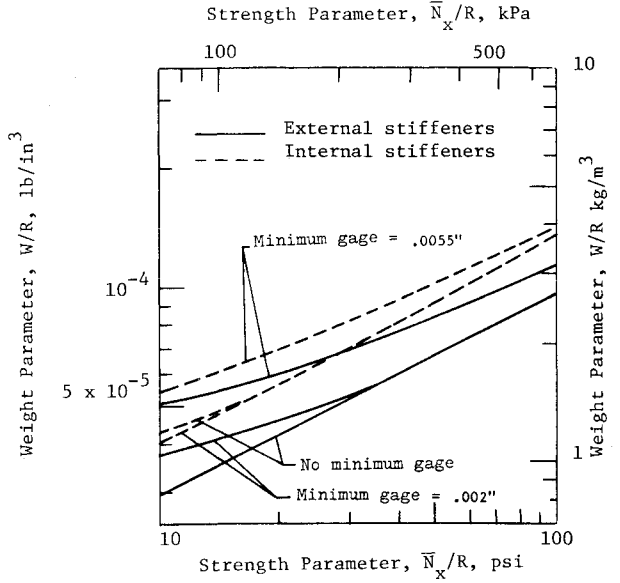

Fig. 9 Weight-strength plot for graphite/epoxy hat-stiffened cylinder with different minimum gage constraints.

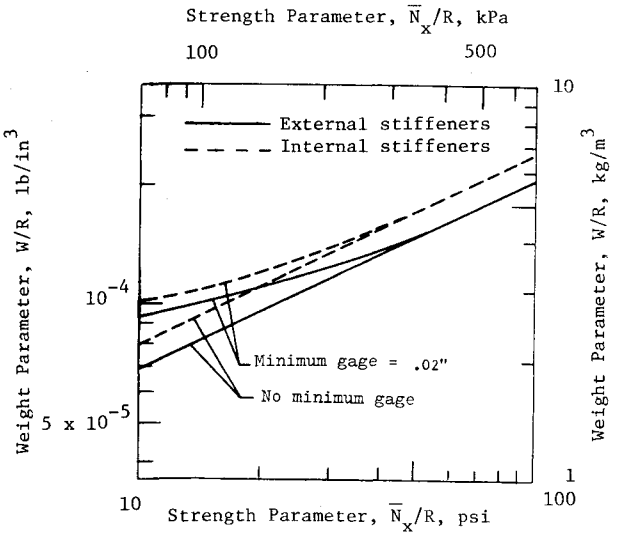

Fig. 10 Weight-strength plot for aluminum hat-stiffened cylinder with different minimum gage constraints.

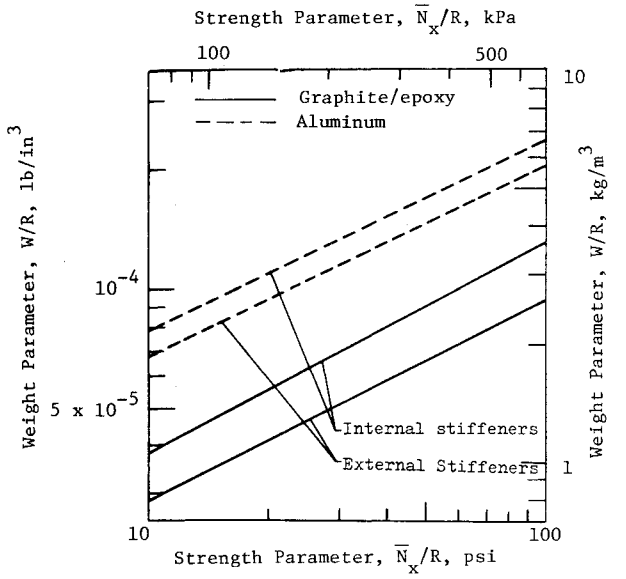

Fig. 11 Comparison of the efficiency of graphite/epoxy and aluminum stringer-stiffened cylinder under axial compression without any minimum gage constraints.

Results for the stringer-stiffened graphite/epoxy cylinder under uniaxial compression are presented in Fig. 9. From the figure, it can be seen that satisfaction of the minimum gage requirement results in a considerable weight penalty for both the externally stiffened and internally stiffened cylinders. The externally stiffened graphite/epoxy cylinders without any minimum gage constraints are about 25% lighter than the corresponding internally stiffened cylinders. But when the minimum gage constraint of 0.0055 in. lamina thickness (0.022 in. laminate thickness) is imposed, the externally stiffened graphite/epoxy cylinders are only about an average of 10% lighter than the corresponding internally stiffened cylinders.

The weight-strength results for the stringer-stiffened aluminum cylinder are presented in Fig. 10. This figure shows that there is a similar weight penalty as shown in Fig. 9 for graphite epoxy cylinder due to the specification of a minimum gage constraint, especially for lower values of the loading parameter $\bar{N}_x/R$. The externally stiffened aluminum cylinders are, respectively, approximately 10 and 15% lighter than the internally stiffened cylinders with and without any imposed minimum gage constraints.

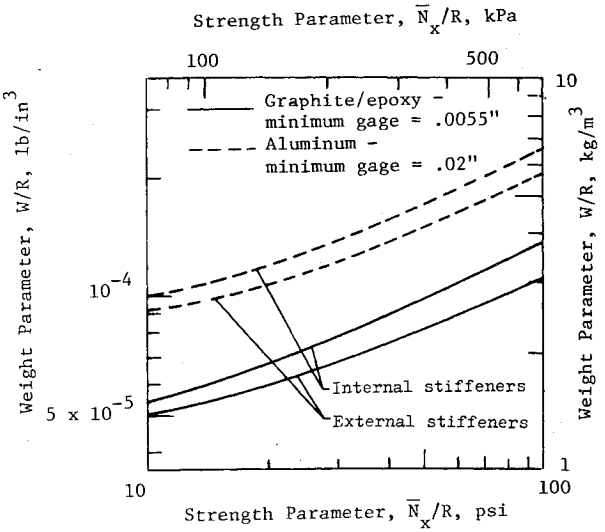

Fig. 12 Comparison of the efficiency of graphite/epoxy and aluminum stringer-stiffened cylinder under uniaxial compression with practical minimum gage constraints.

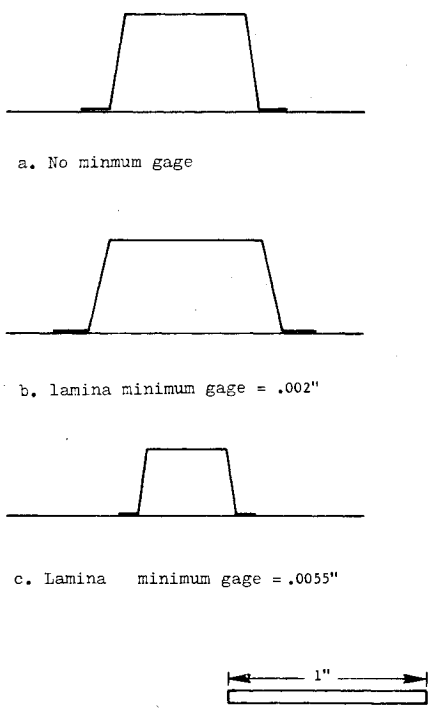

Fig. 13 One pitch cross-sectional dimensions for externally stiffened graphite/epoxy cylinder ($\bar{N}_x/R = 20$ psi, $R = 40$ in., $L = 30$ in.).

Weights of aluminum and graphite/epoxy stringer stiffened cylinders are compared in Figs. 11 and 12. In Fig. 11, no minimum gage constraints are imposed, but in Fig. 12 a lamina minimum gage of 0.0055 in. (0.022 in. laminate minimum gage) for graphite/epoxy cylinders and a laminate minimum gage of 0.02 in. for the aluminum cylinders are imposed. For cases with and without minimum gage constraints, these figures show that the use of a graphite/epoxy cylinder, instead of the aluminum one, results in a weight savings of about 50%. The effect of the change in stringer dimensions for different minimum gage constraints is shown in Fig. 13.

D. Weight Comparison of the Three Basic Configurations

The weight comparison of axially compressed unstiffened, stiffened, and honeycomb sandwich cylinders made from graphite/epoxy and aluminum are shown in Figs. 14 and 15.

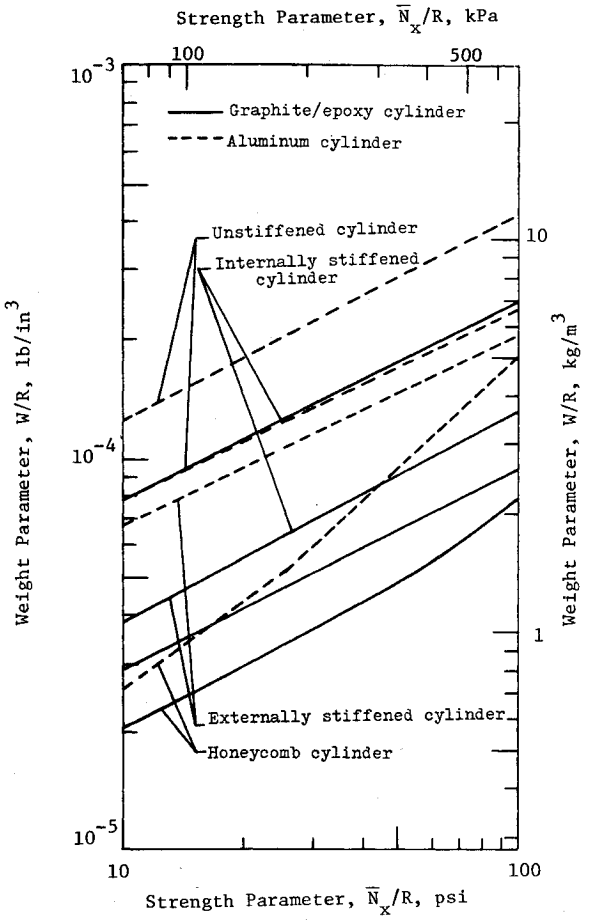

Fig. 14 Weight comparison of three basic cylindrical shell configurations without minimum gage constraints.

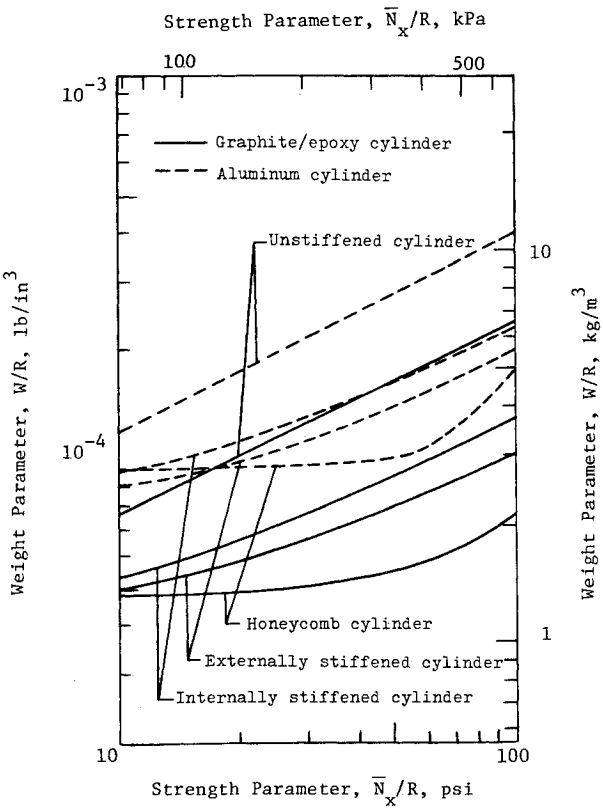

Fig. 15 Weight comparison of three basic cylindrical shell configurations with minimum gage constraints (aluminum minimum gage = 0.02 in., graphite/epoxy lamina minimum gage = 0.0055 in.).

For the case of no minimum gage constraints, Fig. 14 shows for the range of the loading index $\bar{N}_x/R$ considered, which is representative of most aerospace applications, that the honeycomb sandwich cylinder is the most efficient one. It is also interesting to note from Fig. 14 that the unstiffened graphite/epoxy cylinder weighs almost the same as the internally stiffened aluminum cylinder. However, it should be noted that in the results presented here, no "knockdown" factors are included to account for the differences between experimental and the theoretical results of similar configurations. With the inclusion of these knockdown factors, the unstiffened graphite/epoxy cylinders would weigh more than the stiffened aluminum cylinders.

The optimum weight comparisons of unstiffened, stiffened, and honeycomb cylinders with practical minimum gage constraints (0.02 in. for aluminum and 0.0055 in. lamina minimum gage for graphite/epoxy) are shown in Fig. 15. However, no minimum gage constraints have been imposed for the unstiffened cylindrical configuration. Figure 15 shows that the big weight advantage shown by the honeycomb cylinders without the minimum gage requirement is reduced if this requirement is imposed. The weight advantage of the lightly loaded cylinders is effected the most.

IV. Concluding Remarks

This study presents weight-strength plots for three optimized cylindrical shell configurations, namely stiffened, unstiffened, and honeycomb sandwich, with and without practical constraints. These weight-strength plots for graphite/epoxy cylinders are of considerable importance in a comparison of the efficiency of composite materials against conventional aerospace metals. The present approach to the minimum weight design of cylinders under axial compression has resulted in more efficient, theoretically correct, and practical designs than those predicted in previous investigations. It has been shown that the use of graphite/epoxy in the construction of cylinders can save as much as 50% in weight when compared with similar aluminum cylinders. The available minimum gage requirements for the materials impose a significant weight penalty, especially for the lightly loaded cylinders. The use of thinner gage graphite/epoxy (which is available but not very economical) may be desirable for certain applications.

In the use of smeared and conventional discrete stiffener theory for the prediction of buckling loads for composite-stiffened cylinders, the stiffener cross-sectional deformations cannot be ignored as has been done in the past for some metal cylinders. Even for the metal cylinders, the exclusion of such deformations can result in a significant error in the calculation of the buckling load. Cross-sectional deformations of stiffeners have been shown to result in a significantly reduced effective torsional stiffness. Inclusion of the effects of reduced torsional stiffness directly into the optimization process has a very small effect on the overall weight of the stiffened cylinder because the stiffener geometry changes to effect an optimum solution.

The effects of laminated wall construction in the calculation of the bending stiffness matrix for unstiffened composite cylinders under axial compression cannot be ignored as it can result in as much as 20% error in the calculation of the buckling load.

The results presented here show that the use of graphite/epoxy cylinders results in a considerable weight savings in comparison with the weight of corresponding aluminum cylinders, and hence they should be attractive for aerospace applications.

Appendix: Calculation of Stringer Stiffness Properties

Equation (1) requires knowledge of the stiffness properties of the stringers. These properties are determined in this Appendix. Three members of the stiffener, each having a width b_i are shown in Fig. 2. The width of each element is given by

$$b_1 = 0.4b_s$$

$$b_2 = (h_s - \bar{t}_s)/\cos\beta$$

$$b_3 = 0.8b_s \tag{A1}$$

where

$$\bar{t}_s = (t_{sk} + t_{1s} + t_{2s})/2$$

and

$$\tan\beta = 0.1b_s/h_s$$

If $[A]_i$ is the extensional stiffness matrix for the ith member, then Young's modulus E_{x_i} for the ith member in the x direction is given by[18]

$$E_{x_i} = [A_{11} - (A_{12}^2/A_{22})]_i (1/h_i) \tag{A2}$$

where h_i, the thickness of the ith member, is given by

$$h_1 = t_{1s} + t_{2s}$$

$$h_2 = t_{2s}$$

$$h_3 = t_{2s} + t_{3s} \tag{A3}$$

Let EA_i denote the extensional stiffness of each stiffener member. Then the total extensional stiffness of the stiffener E_sA_s is

$$E_sA_s = 2EA_1 + 2EA_2 + EA_3 \tag{A4}$$

where

$$EA_i = E_{x_i} b_i h_i \quad (i = 1,2,3)$$

The distance of the stiffener neutral axis from the skin reference axis $\bar{z}_s$ is given by

$$\bar{z}_s = \frac{2EA_1\bar{t}_s + EA_2(h_s + \bar{t}_s) + EA_3h_s}{E_sA_s} \tag{A5}$$

The bending stiffness E_sI_{os} about the skin reference axis, is given by

$$E_sI_{os} = \frac{EA_1h_1^2}{6} + \frac{E_{s_2}t_{2s}b_s^3\cos^2\beta}{6} + \frac{EA_3h_3{}^2}{12}$$

$$+ 2EA_1\bar{t}_s^2 + 2EA_2\left(\frac{h_s + \bar{t}_s}{2}\right)^2 + EA_3h_s^2 \tag{A6}$$

The torsional stiffness G_sJ_s of the stiffener is computed as follows. From Ref. 19 the torsional stiffness of a closed section isotropic stiffener is given by

$$\frac{1}{GJ} = \frac{1}{4GA^2}\sum_{i=1}^{n}\frac{b_i}{t_i} \tag{A7}$$

where A is the cross-sectional area enclosed by the section, b_i is the width of each element, t_i is the thickness of each element, n is the total number of elements in the section, G is the shear modulus, and GJ is the torsional stiffness. Through the modification of Eq. (A7) for the composite stiffener of

Fig. 5, the above equation becomes

$$\frac{1}{G_s J_s} = \frac{1}{4A^2} \sum_{i=1}^{n} \frac{b_i}{(A_{66})_i} \tag{A8}$$

where $(A_{66})_i$ is the shear stiffness of the ith element. Upon substitution of the indicated values, Eq. (A8) now becomes

$$\frac{1}{G_s J_s} = \frac{1}{4(0.9b_s h_s)^2} \left[\frac{2b_2}{(A_{66})_2} + \frac{b_3}{(A_{66})_3} + \frac{b_s}{(A_{66})_{sk}} \right] \tag{A9}$$

The inplane shear stiffness of the cylinder skin is increased by the presence of the stiffeners, and hence the A_{66} term in Eq. (1) has to be modified accordingly. By neglection of the shear stiffness of the 0° lamina, the inplane shear contribution A_{66}, due to the stringers, is given by[11]

$$A_{66_s} = (A_{66})_2 \left(\frac{0.8b_s \cos\beta + h_s \sin\beta}{0.8b_s \cos\beta + h_s} \right) \frac{1.8b_s}{l_s} \tag{A10}$$

Acknowledgment

The work reported herein was performed under NASA Grant NGR36-004-065 to the University of Cincinnati.

References

[1] Agarwal, B. and Davis, R. C., "Mininum Weight Designs for Hat-Stiffened Composite Panels Under Uniaxial Compression," NASA TN-D 7779, 1974.

[2] Agarwal, B. and Sobel, L. H., "Optimization of a Corrugated Stiffened Composite Panel Under Uniaxial Compression," NASA CR-132314, 1973.

[3] Williams, J. G. and Mikulas, M. M. Jr., "Analytical and Experimental Study of Structurally Efficient Composite Hat-Stiffened Panels Loaded in Axial Compression," ASME/AIAA/SAE 16th Structures, Structural Dynamics, and Materials Conference, Denver, Colo., May 1975.

[4] Michell, A.G.M., "The Limits of Economy of Material in Frame-Structures," *Philosophy Magazine and Journal of Science*, Vol. VIII, July-Dec. 1904.

[5] Crawford, R. F. and Burns, A. B., "Minimum Weight Potentials for Stiffened Plates and Shells," *AIAA Journal*, Vol. 1, April 1963, pp. 879-886.

[6] Gerard, G., "Optimum Structural Design Concepts for Aerospace Vehicles," *Journal of Spacecraft and Rockets*, Vol. 3, Jan. 1966, pp. 5-18.

[7] Morrow, W. M. and Schmit, L. A. Jr., "Structural Synthesis of a Stiffened Cylinder," NASA CR-1217, 1968.

[8] Chao, T. L., "Minimum Weight Design of Stiffened Fiber Composite Cylinders," Ph.D. Thesis, Case Western Reserve University, Dept. of Civil Engineering, 1969.

[9] Kicher, T. P., "Structural Synthesis of Integrally Stiffened Cylinders," *Journal of Spacecraft and Rockets*, Vol. 5, Jan. 1968, pp. 62-67.

[10] Hague, D. S. and Glatt, C. R., "A Guide to the Automated Engineering and Scientific Optimization Program," AESOP. NASA CR-73200, 1968.

[11] Block, D. L., Card, M. F., and Mikulas, M. M. Jr., "Buckling of Eccentrically Stiffened Orthotropic Cylinders," NASA TN-D 2960, 1965.

[12] Viswanathan, A. V. and Tamekuni, M., "Elastic Buckling Analysis for Composite Stiffened Panels and Other Structures Subjected to Biaxial Inplane Loads," NASA CR-2216, 1973.

[13] Agarwal, B. L. and Sobel, L. H., "Minimum Weight Design of Axially Compressed Unstiffened and Stiffened Composite Cylinders," Ph.D. Thesis, University of Cincinnati, Dept. of Aerospace Engineering, 1975.

[14] Bushnell, D., "Evaluation of Various Analytical Models for Buckling and Vibration of Stiffened Shells," *AIAA Journal*, Vol. 11, Sept. 1973, pp. 1283-1291.

[15] Timoshenko, S., *Theory of Elastic Stability*, McGraw-Hill, New York, 1936.

[16] Viswanathan, A. V., Tamekuni, M., and Baker, L., "Elastic Stability of Laminated, Flat and Curved, Long, Rectangular Plates Subjected to Combined Inplane Loads," NASA CR-2216, 1973.

[17] Dow, N. F. and Rosen, B. W., "Structural Efficiency of Orthotropic Cylindrical Shells Subjected to Axial Compression," *AIAA Journal*, Vol. 4, March 1966, pp. 481-485.

[18] Ashton, J. E., Halpin, J. C., and Petit, P. H., *Primer on Composite Materials*, Analysis Technomic Publishing Co., Stamford, Conn., 1969.

[19] Timoshenko, S., *Strength of Materials, Part II*, Van Nostrand, Inc., New York, 1941.